GLOBAL JOURNAL OF PURE AND APPLIED SCIENCES VOL 16, NO. 3, 2010: 333-344
 ISSN 1118-057
www.globaljournalseries.com; Email: info@globaljournalseries.com

NUMERICAL TWO-DIMENSIONAL NATURAL CONVECTION IN AN AIR FILLED SQUARE ENCLOSURE, TILTED (25° AND 65°) IN RELATION TO THE HORIZONTAL PLANE, HEATED FROM TWO OPPOSITE SIDES FOR RAYLEIGH NUMBERS RANGING BETWEEN 10^3 AND 2.10^6

F. P. KIENO AND A. OUÉDRAOGO

(Received 9 December 2008; Revision Accepted 2, December 2009)

ABSTRACT

Steady and transient laminar two-dimensional natural convection of a Newtonian fluid in an inclined square enclosure was numerically investigated. The enclosure was heated on the opposite sides while it was cooled on the other two sides. The inclined angles were 25° and 65° to the horizontal plane. The effect of Rayleigh numbers ranging between 10^3 and 2.10^6 on the flow development and heat transfer was studied. It was found that Nusselt number increases with the increase of Rayleigh number. Under low Rayleigh numbers the numerical studies predict the onset of stationary bi-cellular flow. The study showed that when the Rayleigh number was increased, an overcritical Hopf bifurcation transformed the fixed point to a limit cycle and the steady-state flow becoming oscillatory.

KEYWORDS: Natural Convection, Closed Enclosure, Bifurcations, Limit Point, Limit Cycle, Tilt Angle.

Nomenclature
Latin symbols

a thermal diffusivity [$m^2.s^{-1}$]
dt nondimensional time step
g gravitational acceleration [$m.s^{-2}$]
H height of the cavity [m]
n number of iterations
Nu_c global Nusselt number on the sides AB and CD [$\int_0^1 (\partial T/\partial y)_{y=0}.dx + \int_0^1 (\partial T/\partial y)_{y=1}.dx$]
$\overline{Nu}$ mean Nusselt number
Nx number of nooses in the Ax direction
Ny number of nooses in the Ay direction
Pr: Prandtl number [ν/a]
Ra Rayleigh number [$g\beta(T_h^* - T_c^*).H^3/(\nu.a)$]
Rac critical Rayleigh number
t nondimensional time [t^*a/H^2]
u nondimensional x direction velocity [$u^*.a/H$]

α inclination angle of side AB in relation to the horizontal axis [rad].
β coefficient of thermal expansion [1/K].
λ thermal conductivity [$W.m^{-1}.K^{-1}$]
ν cinematic viscosity [$m^2.s^{-1}$].
ψ nondimensional stream function [ψ^*/a].
ω nondimensional vorticity [$\omega^*.H^2/a$].

Subscripts:
c cold surface.
h hot surface.
m middle
max maximum.
min minimum
0 initial value

Superscripts
* Dimensional quantity

INTRODUCTION

Natural convection in rectangular enclosures has been widely studied both numerically and experimentally due to its applications in numerous natural phenomena such as field temperature prediction in buildings and in industrial processes such cooling of electronics fittings. Natural convection steps as in thermal insulation of buildings with hollow bricks and doubling glazing, flat-plate collectors, cooling by natural radiation.

Studies are numerical or experimental. Important reviews of such heat and mass transfer have been presented and discussed by Ostrach S, Bejan A., Yang K. T. and Berger P.

The most studied cases are rectangular cavities with one wall heated, the opposite side maintained cold and the two remaining sides assumed perfectly

convection in a rectangular cavity at tilted angle 0° and 1° in relation to the horizontal plane and differentially heated. They obtained a pitchfork bifurcation. Chen J. C. et al studying natural convection in a rectangular cavity heating from below and cooling from ceiling with adiabatic sides showed that at low Grashof Gr numbers

heat transfer in a square enclosure tilted at 45° in

F. P. Kieno, Unit of Formation and Research in Exact and Applied Sciences, University of Ouagadougou, 03 BP 7021 Ouagadougou 03, Burkina Faso
A. Ouédraogo, Unit of Formation and Research in Exact and Applied Sciences, University of Ouagadougou, 03 BP 7021 Ouagadougou 03, Burkina Faso

relation to the horizontal plane, heated from the opposite sides and cooled on the other. They showed that the larger the Rayleigh number is, the more sensitive the attractor becomes to time steps and mesh grids. The attractor bifurcates from a limit point to a limit cycle via an overcritical Hopf bifurcation for a Rayleigh number value between $1,11.10^5$ and $1,12.10^5$. For tilt angle of 25° or 65°, the attractor bifurcates from a limit point to a limit cycle via an overcritical Hopf bifurcation for a Rayleigh number value equal 2.10^6.

Hamady F. J. et al studied numerically and experimentally the local natural convection in an air-filled differentially heated inclined enclosure for Rayleigh number between 10^4 and 10^6. Measurements of local and mean Nusselt numbers are obtained at various inclination angles ranging between 0° (heated from above) and 180° (heated from below). They showed that the heat flux at the hot and cold boundaries had a strong dependence on the angle of inclination and the Rayleigh number.

In this investigation, natural convection in enclosure with aspect ratio 1 at inclined angle 25° and 65° were solved numerically by formulation the equations of transfer, of the vorticity and the stream function by central finite-difference (CFD) discretization, which are then solved by using an alternate direction implicit method (ADI).

2 MATHEMATICAL FORMULATIONS

The system under study is an air-filled square enclosure with vertical square section. **Figure1** depicts its transversal section along the Cartesian coordinates (A, x, y). This enclosure is assumed to be very elongated along the horizontal Az direction and perpendicular to the right section. Its sides are inclined at an angle α = 25° or α = 65° with the horizontal plane.

Initially, the system is in thermodynamic equilibrium at temperature T_c. At an initial time t_0, two opposite walls are raised to a warm temperature T_h while the sides BC and AD were maintained at a temperature T_c with $T_h > T_c$. We assume that the fluid is Newtonian and incompressible. All the physical properties of the fluid are constant except the density in the buoyancy term, witch obeys the Boussinesq approximation so that the Prandlt number of air is fixed to 0.71. Radiation, viscous dissipation and pressure effects in the heat transfer equation were negligible. Under the above assumptions, the dimensionless unsteady governing equations in terms of temperature (T), vorticity (ω) and stream function (ψ), using the Cartesian coordinate system are:

- Heat equation*:*

$$\frac{\partial T}{\partial t} + \frac{\partial (uT)}{\partial x} + \frac{\partial (vT)}{\partial y} = \frac{\partial^2 T}{\partial x^2} + \frac{\partial^2 T}{\partial y^2} \qquad (1)$$

- Vorticity equation

$$\frac{\partial \omega}{\partial t} + \frac{\partial (u\omega)}{\partial x} + \frac{\partial (v\omega)}{\partial y} = Ra.\Pr[\cos\alpha \frac{\partial T}{\partial x} - \sin\alpha \frac{\partial T}{\partial y}] + \Pr[\frac{\partial^2 \omega}{\partial x^2} + \frac{\partial^2 \omega}{\partial y^2}] \qquad (2)$$

- Stream function equation:

$$\frac{\partial^2 \psi}{\partial x^2} + \frac{\partial^2 \psi}{\partial y^2} = -\omega \qquad (3)$$

-boundary conditions:

These equations are to be completed with the appropriate boundary and initial conditions.

Initial conditions ($t \le t_0$):

U = 0 ; v= 0 ; ψ = 0 ; T = 0 (4)

U = 0; v = 0; ψ = 0 and T =1 (5)

Conditions at BC and AD (for $t > t_0$): for 0 < y < 1; x = 0 and x = 1

U = 0; v = 0 ; ψ = 0 and T = 0 (6)

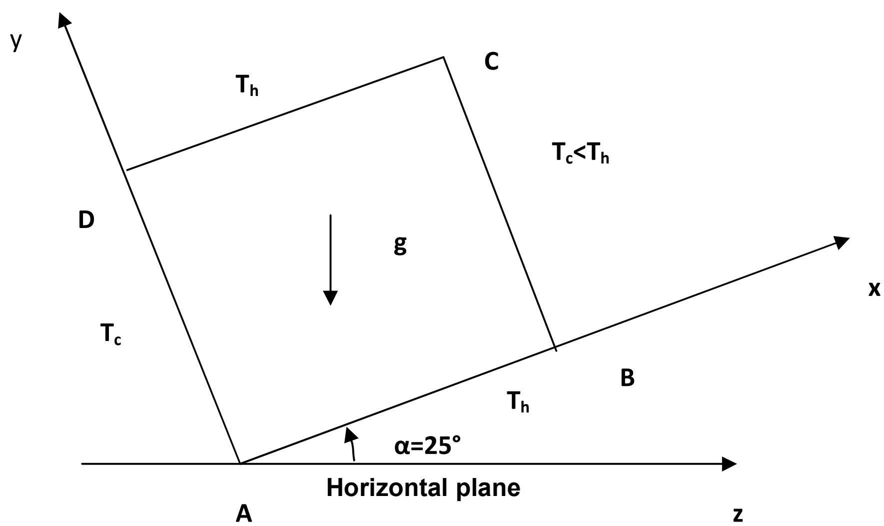

Figure 1: Schematic representation of the system section in the Cartesian frame (A, x, y) at 25° angle tilt.

3 NUMERICAL RESOLUTION METHOD

The differential system (1 – 6) is solved using finite difference method. The discretization scheme used is centred for the space derivative and first order forward for the time derivatives. The wall condition on the vorticity function is evaluated by extrapolation on the internal nodes according to the technique of Woods. The discretized forms of the temperature and vorticity equations are solved by means of an implicit method with alternate directions (A.D.I.) associated with the Gauss elimination method. The stream function is obtained by solving the equation (3) using a successive over relaxation method (S.O.R.) and the velocity field is inferred from stream function.

At each iteration, the test of onvergence is

$$\frac{\sum_i \sum_j \left|\psi^{n+1}(i,j)-\psi^{n}(i,j)\right|}{\sum_i \sum_j \left|\psi^{n+1}(i,j)\right|}<10^{-6} \text{ for stream function.}$$

A same criterion has been imposed on temperature and vorticity.

For temperature the test of convergence is $\dfrac{\sum_i \sum_j \left|T^{n+1}(i,j)-T^{n}(i,j)\right|}{\sum_i \sum_j \left|T^{n+1}(i,j)\right|}<10^{-5}$,

and for vorticity the test of convergence is:

$$\frac{\sum_i \sum_j \left|\omega^{n+1}(i,j)-\omega^{n}(i,j)\right|}{\sum_i \sum_j \left|\omega^{n+1}(i,j)\right|}<10^{-5}.$$

All calculations are carried out in double precision. The reliability of the computer code was established by comparing with the results of G. De Vahl Davis when the attractor was a fixed point (**Table1**). The cavity is vertical and heated differentially along the two vertical walls. The other two horizontal walls are insulated. This table shows that our results are most near of those obtained by G. De Valh Davis. The relative incertitude is below 1%. When the Rayleigh number increases, space mesh must be tightened to obtain good results as those of G. De Valh Davis

Table 1: Results obtained by G. De Vahl Davis and those of present calculations.

Variables	Authors	Ra = 10^3	Ra = 10^4	Ra = 10^5	Ra = 10^6
$Nusselt_{global}$	De Vahl Davis	1,116	2,234	5,512	8,798
	Present calculation	0,75%	0,14%	0,29%	0,97%
		1,1077	2,2372	5,5252	8,8844
Psi_{max}	De Vahl Davis	1,174	5,098	9,644	16,961
	Present calculation	0,03%	0,52%	0,23%	0,19%
		1,1736	5,0717	9,6662	16,993
$Psi_{max,middle}$	De Vahl Davis	1,174	5,098	9,142	16,53
	Present calculation	0,03%	0,52%	0,16%	0,44%
		1,1736	5,0717	9,1277	16,457
$Vx_{max,middle}$	De Vahl Davis	3,679	19,509	68,22	216,75
	Present calculation	0,08%	0,49%	0,30%	0,18%
		3,6819	19,413	68,013	217,14
$Vy_{max,middle}$	De Vahl Davis	3,629	16,182	34,81	65,33
	Present calculation	0,37%	0,40%	0,25%	0,68%
		3,6426	16,117	34,723	64,891

4 RESULTS AND DISCUSSION

4.1 Choice of space mesh and time step

At first time we have made calculations to test the sensibility of solutions to space mesh and time step for various Rayleigh numbers. **Table 2** and **figure 2** show the influence of space mesh for time step dt = 10^{-5}. **Table 2** assembles the values of global Nusselt number Nu_h on hot walls, on cold walls Nu_c, maximal stream function Psi_{max}, minimal stream function Psi_{min}, central stream function Psi_m and central temperature T_m for different space mesh for time step dt = 10^{-5} while **table 3** and **figure 3** show the influence of time step on the same variables.

The calculations show that when the Rayleigh number increases, the results are sensitive to the choice of space mesh and time step. When the solution is stationary, **figures 2** and **3** as **tables 2** and **3** show that the space mesh and the time step can be chosen respectively equal to 141 x141 and 9.10^{-6}.

Table 2: Variations of thermodynamic variables for different space mesh when the Rayleigh number Ra = $1,8.10^6$ and time step dt = 1.10^{-5}. In brackets, the number indicates the relative gap.

Space mesh	Nu_h	Nu_c	Psi_{max}	Psi_{min}	Psi_m	T_m
121x121	0,76%	0,79%	0,57%	0,05%	0,46%	0,00%
	23,134	-23,121	34,669	-27,847	16,080	0,553
131x131	0,72%	0,75%	0,01%	0,03%	0,28%	0,00%
	23,302	-23,297	34,665	-27,838	16,126	0,553
141x141	0,69%	0,69%	0,00%	0,03%	0,25%	0,00%
	23,463	-23,462	34,667	-27,829	16,167	0,553
151x151	0,66%	0,66%	0,00%	0.03%	0,24%	0,00%
	23,619	-23,618	34,666	-27,819	16,206	0,553
161x161	0,59%	0,63%	0,00%	0,02%	0,13%	0,00%
	23,766	-23,768	34,667	-27,814	16,227	0.553
171x171	0,59%	0,59%	0,01%	0,02%	0,18%	0,00%
	23,908	-23,909	34,669	-27,809	16,256	0,553

Table 3: Variations of thermodynamic variables for different values of time step when Ra = $1,8.10^6$ and N_x x N_y = 141 x 141.

Time step	Nu_h	Nu_c	Psi_{max}	Psi_{min}	Psi_m	T_m
1.10^{-5}	23,4634	-23,4623	34,6667	-27,8286	16,1669	0,5527

9.10^{-6}	23,4634	-23,4625	34,6675	-27,8287	16,1627	0,5527
8.10^{-6}	23,4634	-23,4625	34,6673	-27,8286	16,1624	0,5527
7.10^{-6}	23,4634	-23,4625	34,6675	-27,8286	16,1631	0,5527
6.10^{-6}	23,4634	-23,4625	34,6675	-27,8287	16,1633	0,5527

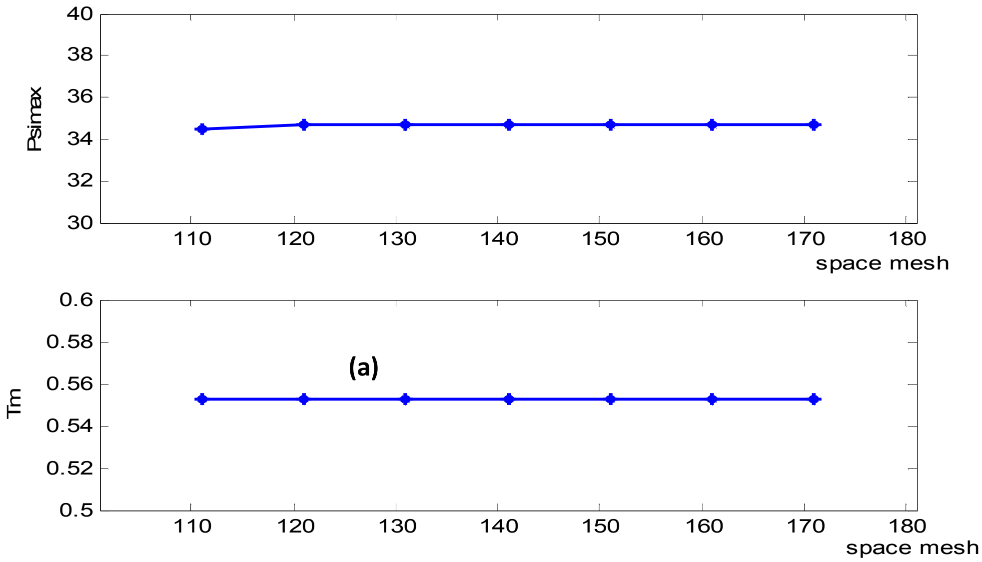

Figure 2: Variations of thermodynamic variables for Ra = $1,8.10^{6}$ and dt = 1.10^{-5}

(a): Influence of the space mesh on Psimax

(b): Influence of the space mesh on Tm

(b)

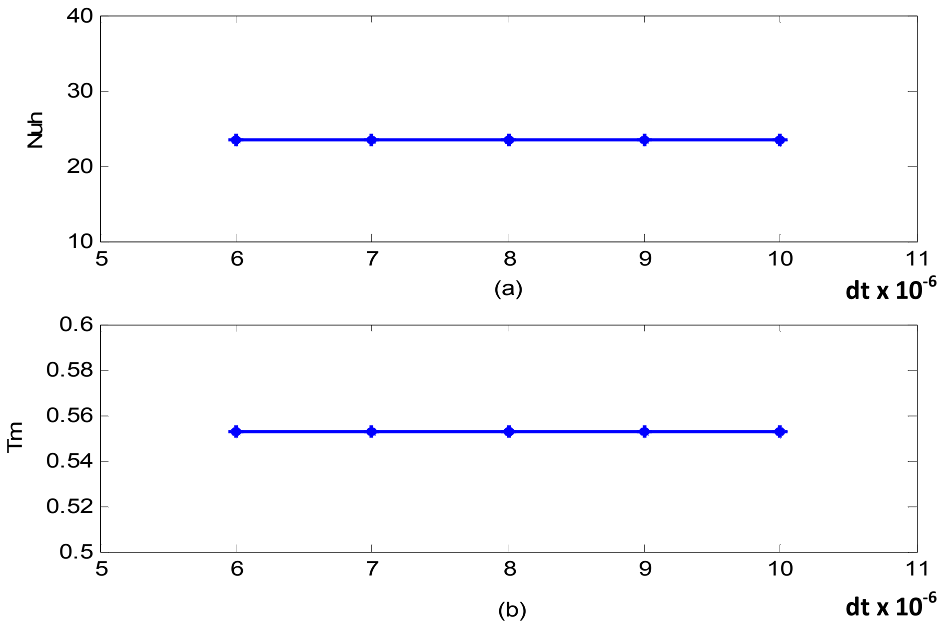

Figure 3: Variations of thermodynamic variables for Ra = 1,8.10^{6} and N_x x N_y = 141 x 141

(a): Influence of the time step on Nu_h

(b): Influence of the time step on Tm

4.2 Fixed point

Even at very low Rayleigh numbers, when the heat transfer is essentially conductive, there is a movement due to the tilt of the walls. The dynamic parameters evolve to a stationary asymptotic limit.

For Ra ≤ 1,95.10^{6}, the thermodynamic parameters evolve at long time towards a stationary asymptotic limit. This behaviour is illustrated on **figure 4** which represents the temporal variation of maximal stream function (a), the trajectory in the phase plane (Psimax, Psi_{min}) (b), the streamlines (c) and the isotherms (d) for Ra = 1,8.10^{6}. We see that the flow involves two cells which rotate in the opposite direction (**figure 4 (c)**). One cell rotates clockwise (negative) while the other rotates counter clockwise (positive). Temporal variations of all parameters converge on a point. All thermodynamic parameters evolve according amortized oscillations before becoming stable at their average value at long time. If one builds up the trajectories of phase of these different parameters, one obtains spirals which start from exterior and lead each one to a point and the attractor is a fixed point.

When Rayleigh number increases from Ra = 1,958.10^{6}, the oscillations of temporal curves dump down more and more with difficulty.

We have also tested the sensibility of the attractor fixed point to initial conditions. **Figures 5 (a)** and **(b)** represent respectively temporal signal of Tm and the trajectory in the phase plane (Psimax, Tm). One shows that the two branches of solutions for **figure 5 (a)** and the three branches of solutions for **figure 5 (b)**, corresponding to initial conditions of very different temperatures at starting, meet at long time.

Progressively that Rayleigh number increases, natural convection expands and thermodynamic parameters increase also except central temperature Tm who decreases. Both temperatures Tm are symmetrical with regard to central temperature T_0 = 0.5 (**Figure 6**).

With complementary inclination angle of 65°, there is symmetry between the two results concerning the streamlines for example (**figure 7**). In case of inclination angle of 65°, one cell rotates clockwise (positive) while the other rotates counter clockwise (negative). These results have been obtained also by Skouta R.

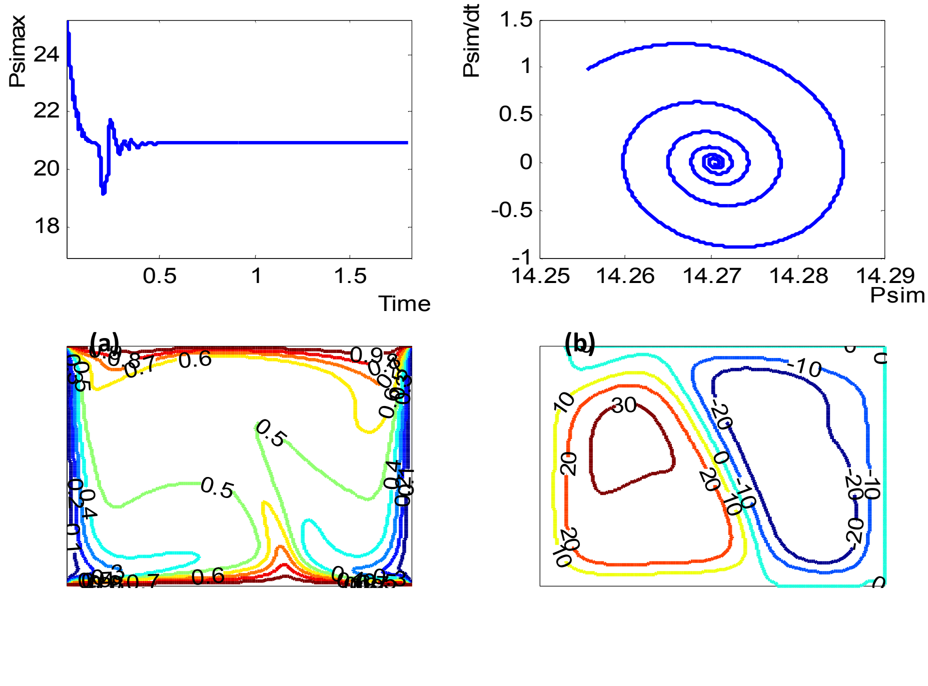

Figure 4: Representation of time evolutions of the maximal stream function (a), of the trajectory in the phase plane (Psim, dPsim/dt), (b), of the streamlines (c) and of the isotherms (d) for Ra = 1,8.10^6

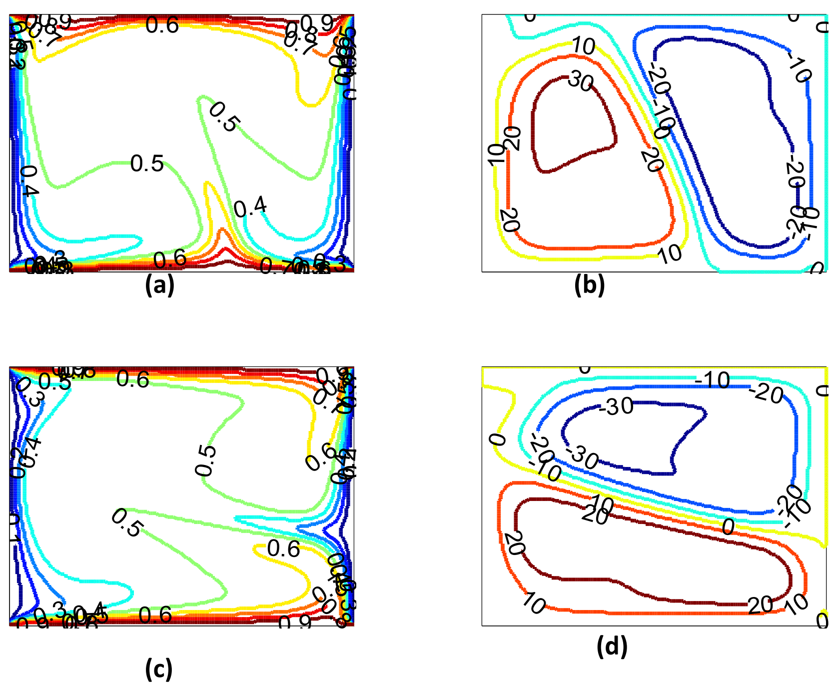

Figure 5: Representation of isotherms (a), (c) and the streamlines ((b), (d) for Ra = 1,8.10^6.

(a), (b): inclination angle α = 25° **(c), (d): inclination angle α = 65°**

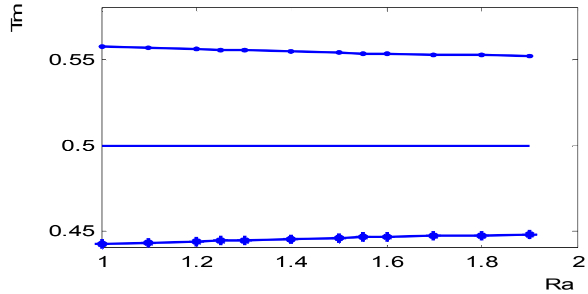

Figure 6: Variations of central temperature versus Ra.10^{-6} for the two tilt angles 25° and 65°

The upper curve corresponds to inclination angle of 25°

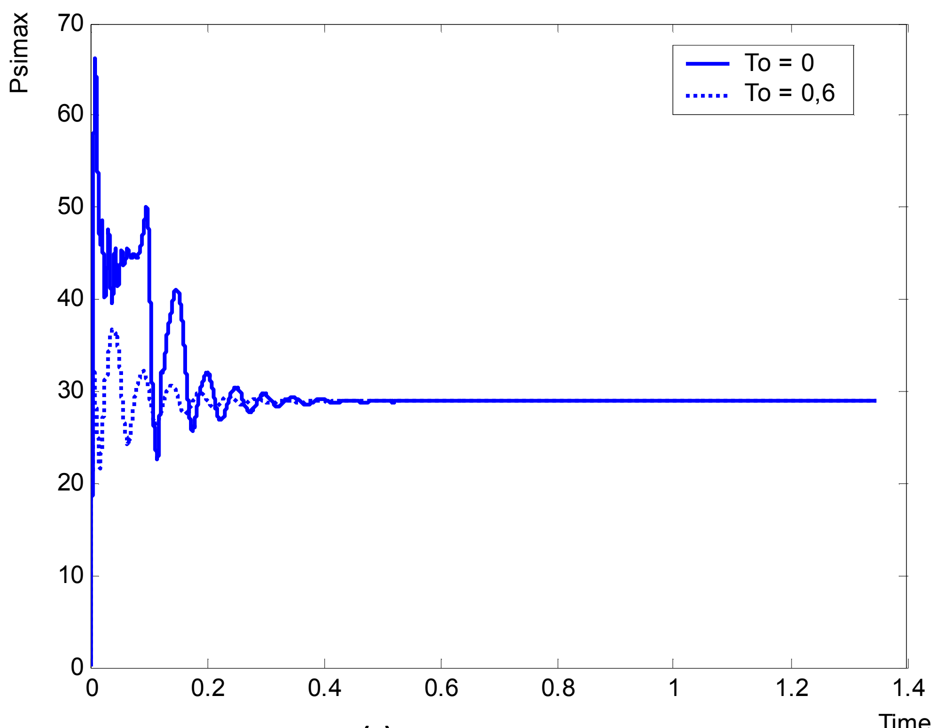

(a)

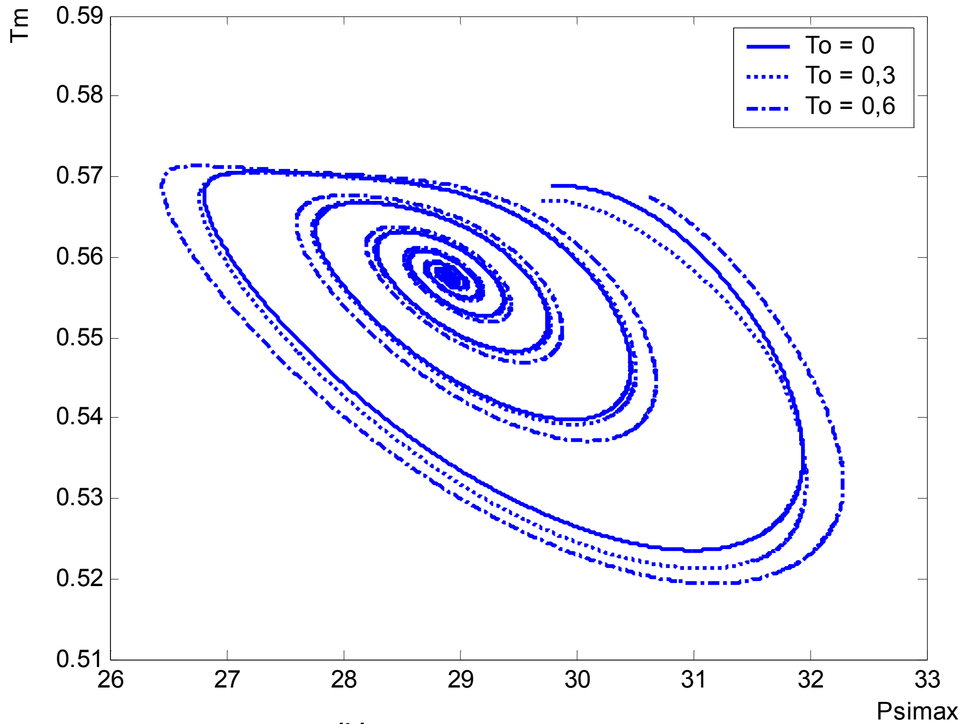

(b)

Figure7 : Nosensitive dependance of attractor on the initial conditions To for Ra = 1,8.10^{6} . (a) Psimax temporal signal; (b) phase plane (Psimax, Tm)

4.3 Hopf bifurcation

For Ra > 1,958.10^{6}, mesh grid was 151 x 151 and dt = 9.10^{-6}. These results have been obtained as we have done in the fixed point case.

When Rayleigh number increases from Ra > 1,958.10^{6}, the flow expands and the computing time necessary to obtain the attractor is increasingly large. There is thus a critical Rayleigh number Ra_c situated in interval [1,958.10^{6}; 1,96.10^{6}] from which the attractor is periodic as one sees on **figure 8** who represents temporal evolution (a), the amplitude spectrum (b) of Tm and the trajectory in the phase plane (Tm, Psim) (c) for Ra = 1,96.10^{6}. The plotting of the amplitude spectrum obtained by Fast Fourier Transform (**Figure 9 (c)**) corroborates the existence of a limit cycle. There is a critical value of the Rayleigh number above which the attractor is periodic and independent of initial conditions (**figure 9 (d)**).

To determine the nature of the phenomenon corresponding to the transition from fixed point to limit cycle, we have studied both the variations of oscillatory amplitude versus the square root of the gap between $(Ra.10^{-6} - Ra_c.10^{-6})^{1/2}$ in witch Ra_c is the critical Rayleigh number and also the variations of the fundamental frequency in vicinity of bifurcation point. **Figure 9** represents the variations of oscillatory amplitude versus $(Ra.10^{-6} - 1,958.10^{-6})$. It shows that the amplitude of cycle is proportional to this gap, witch increases as the square root of the gap at bifurcation point. There two characteristics allow us to conclude that the bifurcation is an over critical Hopf bifurcation.

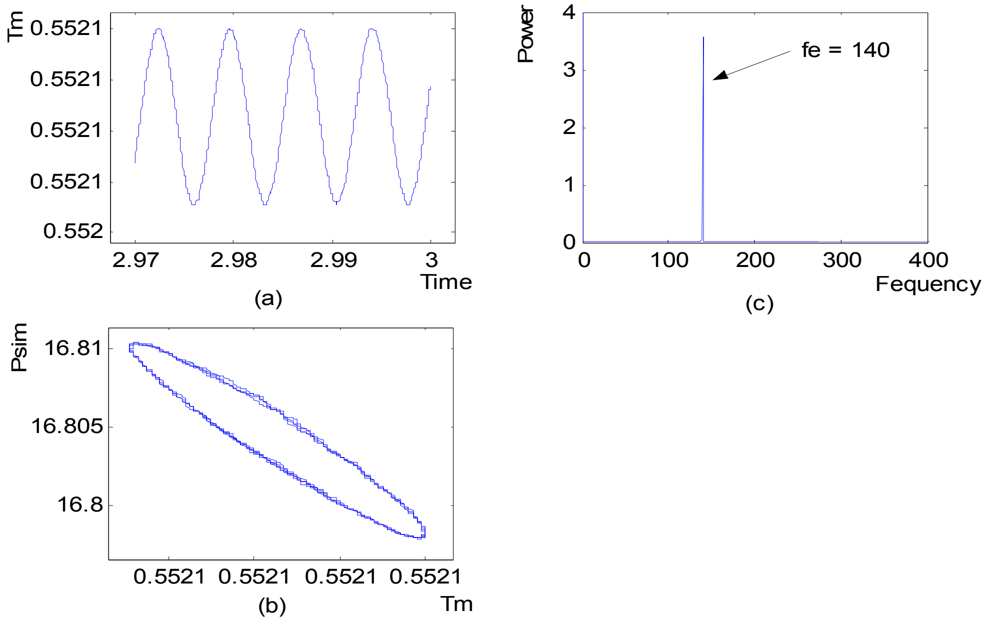

Figure 8 : Illustration of limit cycle for Ra = 1,96.10^{6}

(a): temporal signal of Tm
(b): amplitude spectrum of Tm
(c): trajectory in the (Tm, Psim) phase plane

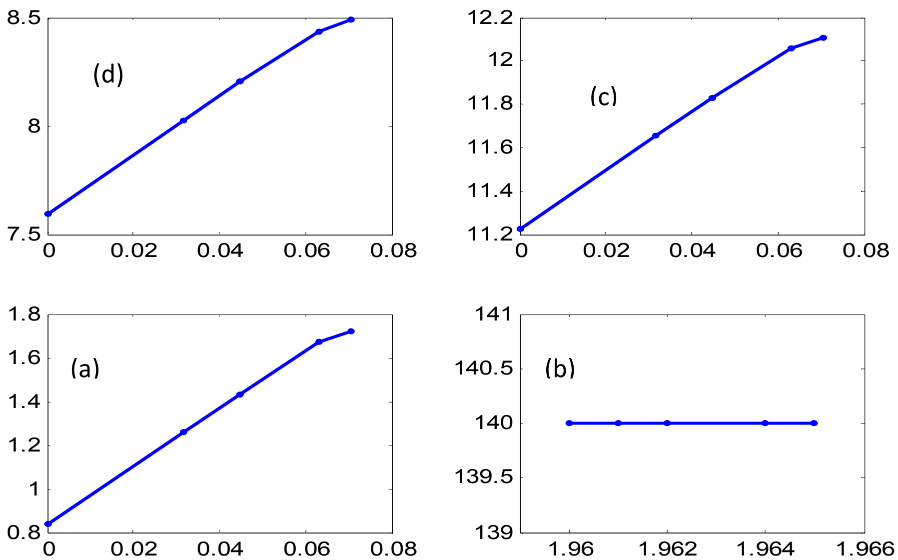

Figure 9: Influence of Rayleigh number in vicinity of bifurcation point

(a) Variation of amplitude of Nu_h versus $(Ra.10^{-6}-1{,}960)^{1/2}$

(d)

(b) Variation of amplitude of Psim versus $(Ra.10^{-6}-1{,}960)^{1/2}$

(c) Variation of amplitude of Tm versus $(Ra.10^{-6}-1{,}960)^{1/2}$

4.4 Mean Nusselt number

At each step time, we have obtained $Nu_h = |Nu_c|$ for the Rayleigh numbers ranging between 1.10^{3} and 2.10^{6} with a precision of 0.03%. We have calculated the mean value $\overline{Nu}$ of both global Nusselt numbers situated in this interval for a few Rayleigh numbers. For the numerical data presented here, the correlation of the mean Nusselt number for the inclined (25°) enclosure as a function of Rayleigh number with an error of the order of 1% is found to be $\overline{Nu} = 1.7178 \times Ra^{0.1818}$

Figure 10 presents the comparison of the global Nusselt number Nu_h obtained by the calculation and the mean Nusselt number $\overline{Nu}$ as a function of Rayleigh number for the inclined (25°) enclosure. The effect of inclination angle on Nusselt number is more pronounced when the Rayleigh number increases. This is due to the fact that when the Rayleigh number increases the convection is the dominant mode of the heat transfer and the orientation of gravity vector with respect to the density gradient in the enclosure influences the convection and heat transfer more.

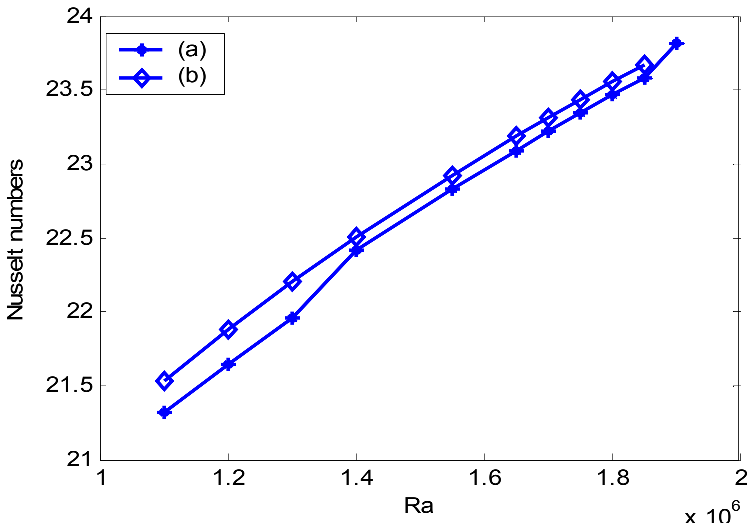

Figure 10: Comparison of mean Nusselt number $\overline{Nu}$ (a) and global Nusselt number Nu_h (b) for α = 25°

5 CONCLUSION

The present study has presented a numerical data showing the influence of inclination on thermodynamic parameters as global Nusselt numbers, stream function and temperatures distributions in the cavity for 25° and 65° tilt angles and Rayleigh number included in the interval [1.10^3, 2.10^6].

The implicit centred finite difference method used, allowed us to find with an excellent agreement the results of the literature concerning problems similar to that considered here when the attractor is a fixed point or limit cycle. Generally, the results are more sensitive to space and time steps when Rayleigh number increases.

It has been shown that when Rayleigh number increases, there is a critical value of it included in the interval [$1,958.10^6$, $1,96.10^6$] where the flow undergoes a Hopf bifurcation.

Theoretically, the routes toward Hopf bifurcation for complementary angles (25 ° and 65° for example) are identical. If the cavity elements of symmetry are considered, it is sufficient to solve the Boussinesq equations for tilt angles included in the interval [0°, 45°].

In general, heat transfer increases with increase in Rayleigh number. From the predicted results, simple correlation for mean Nusselt number as a function of Rayleigh number is obtained for design applications.

ACKNOWLEDGEMENTS

This work was supported by the Coopération Universitaire Institutional, Universités Francophones de Belgique (CIUF) with financial support of the A.G.C.D. The authors like to thank them kindly.

REFERENCES

Bejan, A., 1980. A synthesis of analytical results for natural convection heat transfer across rectangular enclosures, Int. J. Heat and Mass Transfer, 23: 723-726.

De Vahl Davis G., 1968. Laminar natural convection in

De Vahl Davis G., 1982. Natural convection of air in square cavity: a benchmark solution, Int. J. for Numerical Methods in Fluids, 3: 249-264.

Musushima J., Adachi T., 1995. Structural stability of the pitchfork bifurcation of thermal convection in a rectangular cavity, Journal of Physical Society of Japan, 64, (12): 4670-4683.

Ostrach S., 1988. Natural convection in enclosures, Journal of Heat Transfer, 110/1175: 1175-1190.

Skouta A., Randriazanamparany M.A., Daguenet M., 2001. Etude numérique de la convection naturelle instantionnaire bidimensionnelle dans une enceinte allongée, de grand axe horizontal et de section carrée, inclinée eu égard au plan horizontal et chauffée par deux côtés opposés, Int. Journal Thermice Science, (40): pp.352-365.

Sktouta R, Skouta A., Daguenet M., 2008. Numerical study of the transition toward chaos of two dimensional natural convection within an inclined square cavity, Adv, Studies Theor. Phys, 2, 2008, (1): 37–50.

Hamady F. J., Lloyd J. R., Yang H. Q., Yang K. T., 1989. Study of local natural convection heat transfer in an inclined enclosure, Int. J. Heat and Mass Transfer, 32: 1697-1708.

Yang K. T., 1988. Transitions and bifurcations in laminar buoyant flows in confined enclosures**,** Journal of Heat of Heat Transfer, 110: 1191-1204.

Bejan A., 1984. Convection Heat and Mass Transfer, John Wiley and Sons.

Bergé P., Pomeau Y., Vidal C., 1988. L'ordre dans le chaos, vers une approche déterministe de la turbulence, Hermann, Paris.

Ostrach S., 1972. Natural convection in enclosures, Hartnet, Irvine (Eds.) Advances in Heat Transfer, volume 8, Acadamic Press.

Yang K. T., 1987. Natural convection in enclosures, handbook of Single Phase Convection Heat Transfer, John Wiley, New-York, pp.1-51.

Woods L. C., 1954. A note on the numerical solution of fourth order differential equations, Aenauit. Q. 5 (3).